The Clay Minerals Society Workshop Lectures Series, Vol. 21 (2016), Chapter 19, 241–250

CLAY-BASED MODELING APPROACH TO DIFFUSION AND SORPTION IN THE ARGILLACEOUS ROCK FROM THE HORONOBE URL: APPLICATION TO Ni(II), Am(III), AND Se(IV)

YUKIO TACHI*, TADAHIRO SUYAMA, KENJI YOTSUJI, YASUO ISHII, and HIROAKI TAKAHASHI

Japan Atomic Energy Agency, 4-33 Muramatsu, Tokai, Ibaraki, 319-1194, Japan
**e-mail: tachi.yukio@jaea.go.jp*

Sorption and diffusion of radionuclides (RNs) in argillaceous rocks are key processes in the safe geological disposal of radioactive waste. Sorption and diffusion of Ni(II), Am(III), and Se(IV) in mudstone from the Horonobe Underground Research Laboratory were investigated using experimental and modeling approaches. Effective diffusivities obtained by means of through-diffusion experiments were in the following decreasing order: $Cs^{+} > Ni^{2+} \approx HTO > I^{-} > Se\ (SeO_3^{2-}) > Am\ (Am(CO_3)_2^{-})$ based on a comparison with the results of previous studies. The distribution coefficient values were consistent with those obtained using batch sorption tests. These results were interpreted using the clay-based modeling approach coupled with the thermodynamic sorption model by assuming key contributions of clays (smectite and illite), and the diffusion model by assuming the electric double layer theory and the simplified pore model with size distribution. This clay-based model can provide a reasonable account of observed trends for various RNs with complex chemistry, although some systematic gaps in the modeling results need to be evaluated further by considering uncertainties in both the experimental and the modeling approaches.

1. Introduction

Sorption and diffusion of radionuclides (RNs) in argillaceous rocks and compacted clays are key processes in the safe geological disposal of radioactive waste (*e.g.* NEA, 2012). To set reliable parameters under various geochemical conditions relevant to the performance assessment, a detailed understanding of the processes of diffusion and sorption is necessary, as is the development of mechanistic models which describe these processes. Various types of quantitative modeling approaches for both sorption (*e.g.* Bradbury and Baeyens, 2005; Marques Fernandes *et al.*, 2015) and diffusion (*e.g.* Leroy *et al.*, 2006; Appelo *et al.*, 2010) in argillaceous rocks and compacted clays have been developed.

The integrated sorption and diffusion (ISD) model for compacted bentonites has been developed on the basis of consistent combination of sorption and diffusion models, assuming a dominant contribution of montmorillonite to sorption, diffusion, and homogeneous pore distribution in compacted bentonite (Tachi and Yotsuji, 2014; Tachi *et al.*,

DOI: 10.1346/CMS-WLS-21.19

2014a, 2014b). The diffusion model was based on a simplified pore structure and on the electrical double layer (EDL) theory, which describes the change in ionic concentrations and viscoelectric effects due to electrostatic interaction with negatively charged clay surfaces. The sorption trends of various RNs can be described quantitatively by a model that considers a one-site non-electrostatic surface complexation model in combination with the one-site ion-exchange model. The ISD model accounted quantitatively for sorption and diffusion data of various RNs such as cations (Cs^+, Na^+, Sr^{2+}), anions (I^-), and actinide species (Np(V), Am(III), U(VI)) as functions of porewater salinity and dry density (*e.g.* Tachi and Yotsuji, 2014; Tachi *et al.*, 2010, 2014a, 2014b).

This clay-based modeling approach has been extended to describe the sorption and diffusion behavior of simple cations (Cs^+) and anions (I^-) in the more complex argillaceous rock from the Horonobe underground research laboratory (URL) by assuming a simplified pore model and key contributions of clay surfaces (Tachi *et al.*, 2011). One of the key challenges for validating this clay-based modeling approach is testing its applicability to more complex RNs. The present study focused, therefore, on experimental and modeling investigations of the diffusion and sorption of Ni(II), Am(III), and Se(IV) in samples of the argillaceous rock from the Horonobe URL, Japan.

2. Experimental and results

The effective diffusivities (D_e) and distribution coefficients (K_d) of Ni(II), Am(III), and Se(IV) were measured for the rock samples (siliceous mudstone/Wakkanai Formation) from the Horonobe URL which were sampled from the drillcore of borehole HDB-6 at a depth of -500 m and were described in detail previously by Tachi *et al.* (2011). The diffusion tests were conducted using the through-diffusion method based on the procedure described by Tachi *et al.* (2011) under anaerobic conditions at room temperature. The rock samples were pre-saturated with synthetic groundwater (Na^+, K^+, Mg^{2+}, Ca^{2+}, Cl^-, CO_3^{2-}, SO_4^{2-}) with an ionic strength of 0.24 M and pH of 8.5 based on *in situ* groundwater compositions sampled from HDB-6 (JAEA, 2007). Tracer solutions were added as initial concentrations of Ni, Am, and Se, and their values were 1×10^{-6} M, 6×10^{-9} M, and 1×10^{-4} M, respectively. The pH values of the solutions were monitored periodically, and were found to be stable at $\sim$8.5. Tracer concentrations in the inlet and outlet reservoirs were monitored, and depth profiles were measured using the abrasive profiling method described by Tachi *et al.* (2011) after a diffusion period. Batch sorption tests using crushed rock samples (<355 μm) were conducted as a function of pH (5–10) under consistent conditions with a diffusion test. Liquid-to-solid ratios were set taking into account a wide range of K_d values for each tracer: 100 mL/g for Ni, 1 L/g for Am, and 10 mL/g for Se. After 7–28 days of reaction time, tracer concentrations in the 0.45 μm-filtered solution for Ni and Se or the supernatant solution after centrifugation at 6000 rpm for 30 min for Am (centrifugation was selected as an effective separation method for Am based on comparison with filtration) were measured, and K_d values were then determined.

Sets of the tracer-depletion curve in the inlet reservoir, breakthrough curve in the outlet reservoir (for Se only), and the depth profile of the three tracers, are shown in Figure 1. The D_e and K_d values were determined by multiple-curve analysis

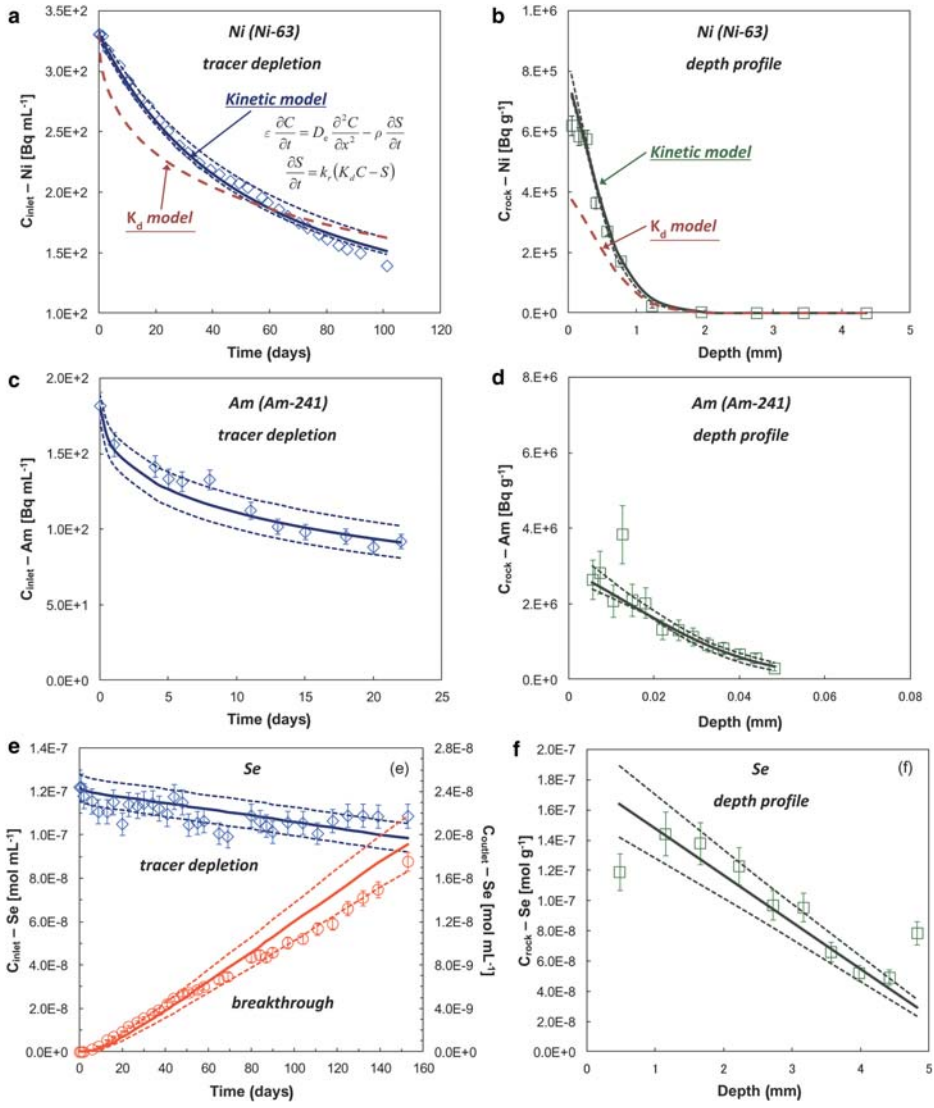

Figure 1. Typical results of through-diffusion experiments for: (a–b) Ni, (c–d) Am, and (e–f) Se(IV). Inlet depletion curves and outlet breakthrough curves are shown in parts a, c, and e, and depth profiles are shown in parts b, d, and f. The solid lines are best-fit curves obtained by simultaneous fitting of the diffusion equations assuming the K_d model (Am and Se) or the kinetics model (Ni). The dashed lines without remarks indicate ranges of uncertainty.

Table 1. Diffusion and sorption parameters of Ni, Am, and Se in rock samples obtained from through-diffusion experiments.

Tracer	D_e ($m^2\ s^{-1}$)	α (−)	K_d ($m^3\ kg^{-1}$)	Remarks
Ni	$(1.27 \pm 0.09) \times 10^{-10}$	–	$(4.87 \pm 0.09) \times 10^{0}$	Kinetics model
	$(1.48 \pm 0.02) \times 10^{-10}$	–	$(3.62 \pm 0.07) \times 10^{0}$	Kinetics model
Am	$(1.25 \pm 0.12) \times 10^{-11}$	$(6.04 \pm 0.86) \times 10^{4}$	$(3.89 \pm 0.55) \times 10^{1}$	K_d model
	$(8.81 \pm 1.46) \times 10^{-12}$	$(9.54 \pm 1.46) \times 10^{4}$	$(6.16 \pm 4.07) \times 10^{1}$	K_d model
Se	$(1.73 \pm 0.15) \times 10^{-11}$	3.28 ± 0.28	$(1.87 \pm 0.18) \times 10^{-3}$	K_d model
	$(1.27 \pm 0.12) \times 10^{-11}$	2.19 ± 0.21	$(1.17 \pm 0.13) \times 10^{-3}$	K_d model

(Tachi and Yotsuji, 2014), and could then be fitted with a conventional diffusion model coupled with the K_d model for Am and Se. Significant disparities between the modeled and measured curves were observed for Ni, however (Figure 1a,b). The diffusion model coupled with a first-order kinetics sorption model was applied on the basis of previous studies (*e.g.* Scheidegger *et al.*, 1998; Strawn and Sparks, 2000), and simulated both the tracer depletion curve and the depth profile reasonably well, as shown in Figure 1a,b. The best-fit sorption and diffusion parameters and their uncertainties are summarized in Table 1.

The D_e values obtained were in the order: $Cs^+ > Ni^{2+}$ $(1.27–1.48 \times 10^{-10}\ m^2/s) \approx$ HTO $> I^- >$ Se $(1.27–1.73 \times 10^{-11}\ m^2/s) >$ Am $(0.88–1.25 \times 10^{-11}\ m^2/s)$, as summarized in Table 1 (Figure 2b). These D_e trends showed typical cation excess and anion exclusion effects in the case of complex species. The diffusion-determined K_d values were in the order: Am $(3.89–6.16 \times 10^{1}\ m^3/kg) >$ Ni $(3.62–4.87 \times 10^{0}\ m^3/kg) >$ Se $(1.17–1.87 \times 10^{-3}\ m^3/kg)$. These K_d values were consistent with those from the batch sorption tests, as shown in Figure 2a. The pH dependences of K_d showed typical trends, as reported previously: K_d increased with increasing pH for Ni (*e.g.* Bradbury and Baeyens, 2005), it decreased with increasing pH for Am because of carbonate effects (*e.g.* Marques Fernandes *et al.*, 2008), and typical K_d reductions were observed with increasing pH for oxyanion-forming Se (*e.g.* Missana *et al.*, 2009).

3. Modeling and discussion

A clay-based modeling approach, assuming key contributions from the clay components (illite and smectite), was proposed to interpret the observed diffusion and sorption behavior of simple cations (Cs^+) and anions (I^-) (Tachi *et al.*, 2011). This modeling approach is applied to the sorption and diffusion results obtained here. For sorption modeling, the component additive (CA) model (NEA, 2012), which includes smectite and illite contents and their sorption model parameters, was applied. Sorption models were developed for smectite and illite systems (Tachi *et al.*, 2014a, JAEA, 2013) based on experimental data from the literature, which had originally been obtained in batch experiments as functions of key geochemical conditions (*e.g.* pH). The models were based on a one-site surface complexation model without electrostatic correction terms and a one-site ion exchange model. All models were parameterized to be

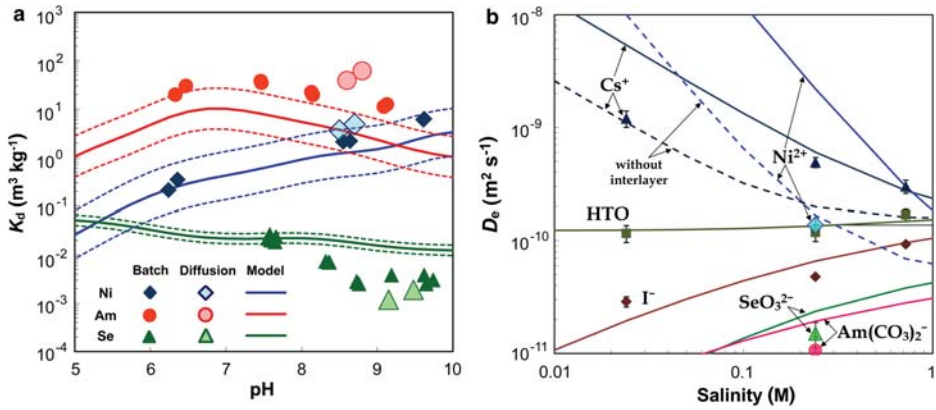

Figure 2. Comparison between measured and modeled results for Ni, Am, and Se: (a) K_d values and modeling result as a function of pH. The solid and dashed lines represent modeled results and uncertainty ranges, respectively. (b) D_e values and modeling result as a function of porewater salinity. The solid lines denote modeled results. The results for Cs, I, and HTO were taken from Tachi *et al.* (2011).

consistent with the JAEA Thermodynamic Database (Kitamura *et al.*, 2010). The sorption-model parameters of Ni, Am, and Se summarized in Table 2 were applied directly to the Horonobe rock system.

K_d values were calculated using the geochemical code, *PHREEQC* (Parkhurst and Appelo, 1999). Key parameters in sorption modeling were the amounts of illite and smectite in the rock sample, set to 10 wt.% for illite and 16 wt.% for smectite, based on mineralogical analyses of the same rock samples (Tachi *et al.*, 2011). The distribution of RNs between the sorption sites (basal and edge planes) and solution was calculated using site capacities determined from the clay contents and sorption parameters. The K_d values of whole-rock samples were then evaluated as the ratio of the quantity of sorbed RNs on all sorption sites of clays (illite and smectite) and the equilibrium concentrations of RNs in solutions. Trends in K_d predicted by the sorption model, considering additive contributions of illite and smectite, showed reasonable agreement with the K_d values measured as a function of pH by batch sorption experiments, as shown in Figure 2a, although systematic discrepancies between the modeled and measured K_d values were observed for Am and Se. In these sorption-model calculations, the dominant species were Ni^{2+}, $Am(CO_3)_2^-$, and SeO_3^{2-}.

Diffusion behaviors were interpreted using the clay-based diffusion model based on a simplified pore structure and the EDL theory, which describes the change in ionic concentration (cation excess and anion deficit) and water viscosity due to electrostatic interaction with negatively charged clay surfaces. The key concept and equations are summarized in Figure 3 (details can be found in Tachi *et al.*, 2011; Tachi and Yotsuji, 2014). Two basic assumptions were made for the application of the ISD model to the more complex argillaceous rock. First, a dominant contribution of clay components (illite and smectite) was assumed for diffusion and sorption modeling.

Table 2. Sorption model parameters of Ni, Am, and Se for smectite and illite (Tachi *et al.*, 2014a; JAEA, 2013).

Smectite model					**Illite model**		
Titration data: Shibutani *et al.* (1999) – CEC; 108 (meq/100g) (fixed) – SOH density; 4.31×10^{-5} (mol/g) – SOH_2^+; 5.75, SO^-; −8.30					Titration data: Bradbury and Baeyens (2009a) – CEC; 22.5 (meq/100g) (fixed) – SOH density; 4.01×10^{-5} (mol/g) – SOH_2^+; 3.84, SO^-; −6.24, ($S'OH_2^+$; 8.45, $S'O^-$; −10.2)		
RNs	**Surface species**		**Smectite: log K**	**Uncertainty**	**Illite: log K**	**Uncertainty**	**Dataset**
Ni	SCM	$SONi^+$	−2.32	0.28	−0.633	0.19	Smectite: Bradbury and Baeyens (2005) Tertre *et al.* (2005) Illite: Bradbury and Baeyens (2009a) Poinssot *et al.* (1999)
		SONiOH	−12.2		−9.26		
		$SONi(OH)_2^-$	−21		−18.5		
	Iex	Z_2Ni	0.7		1.4		
Am (Eu)	SCM	$SOAm^{2+}$	0.304	0.36	1.8	0.5	Smectite: Gorgeon (1994) Marques Fernandes *et al.* (2008) Illite: Bradbury and Baeyens (2009b) Poinssot *et al.* (1999) Rabung *et al.* (2005)
		$SOAmOH^+$	−7.62		−5.88		
		$SOAm(OH)_2$	−16.6		−14.5		
		$SOAm(OH)_3^-$	−27.3		–		
		$SOAmCO_3$	6.74		8.51		
		$SOAm(CO_3)_2^{2-}$	10.4		12.2		
	Iex	Z_3Am	2.1		1.1		
Se	SCM	SOH_3SeO_3	18.1	0.12	–	–	Smectite Missana *et al.* (2009)
		$SOH_2SeO_3^-$	11.7		–		
		$SOHSeO_3^{2-}$	4.26		–		
		$SOSeO_3^{3-}$	−4.62		–		

The rock samples from the Wakkanai Formation consist predominantly (50 wt.% or more) of opal-CT or quartz. As shown in Figure 3a,d (Takahashi *et al.*, 2009), pore spaces between the dominant minerals form homogeneous pore networks which can be identified, using nano X-ray CT, as pores which are greater than sub-micrometer in size (Figure 3d). The pore-size distributions measured by mercury porosimetry, however (Figure 3e), indicated that nm-scale pores ($<$100 nm) are dominant in the rock samples. The above-mentioned diffusion behaviors, especially cation excess and anion exclusion effects, and the pore-size distributions dominated by nm-scale pores, imply that an homogeneously dispersed clay matrix dominates ionic diffusion in these rock samples (Tachi *et al.*, 2011).

Under the second assumption, to extend the EDL diffusion model to more complex argillaceous rocks, characterization of the pore geometry, size distribution, and surface charge of the pore surface are required. The clay matrix consists of different types of clay minerals and pore spaces: non-swelling illite without interlayer water and swelling smectite with interlayer water (Figure 3b). As discussed by Tachi *et al.* (2011), the pore shape can be assumed to be close to parallel plates (Figure 3c), and the pore-size distribution can be evaluated by mercury porosimetry and estimation of interlayer pores ($<$nm), as shown in Figure 3e. In contrast, the surface charge of smectite was used to represent the surface charge density of pores in the diffusion model by considering the maximum smectite content and key contributions of its interlayer pores. The negative surface charge of clays leads to an excess of cations and exclusion of anions; these effects are termed electrostatic constrictivity (δ_{el}) (equation 1 in Figure 3f). δ_{el} is the averaged ratio between ionic concentration in the diffuse layer and that in bulk water, taking into account the enhanced water viscosity due to viscoelectric effects (equations 2–4). The D_e values can be evaluated using a weighted average of δ_{el}, which is determined from the pore-size distribution and δ_{el} at each pore size (equation 5). The total porosity (37.6%) and geometric factor (δ_g/τ^2; 0.14) derived from the D_e values of HTO were used. This value of the geometric factor was reasonably consistent with the value of $1/\tau^2$ (=0.15) determined from 3D image analysis of the pore networks and their medial axis (Figure 3d) extracted from the 3D image by nano-focus X-ray CT (Takahashi *et al.*, 2009). The values of tracer diffusivities in bulk liquid water (D_w) were based on literature data by considering chemical analogs. The other parameters employed in diffusion modeling were described by Tachi *et al.* (2011).

Considering the electrostatic effects averaged using the surface area distribution as a weight fraction, the model can predict the cation excess and anion-exclusion effects, and their dependence on the salinity of synthetic groundwater reasonably well (Cs^+ and I^-; Tachi *et al.*, 2011). The modeled D_e values of Ni^{2+}, $Am(CO_3)_2^-$, and SeO_3^{2-}, which were calculated as dominant species under the geochemical conditions of the diffusion experiments, are shown in Figure 2b and compared with the corresponding measured values. The diffusion model can express qualitatively the cation excess and anion-reduced diffusion ($Cs^+ > Ni^{2+} > HTO > I^- > SeO_3^{2-} > Am(CO_3)_2^-$). To investigate the cause of a significant gap in the case of Ni^{2+}, the modeled results ignoring the contribution of interlayer pores are shown for Cs^+ and Ni^{2+} in Figure 2b. As can be seen in Figure 2b, interlayer pores make a significant contribution to cation diffusion, and

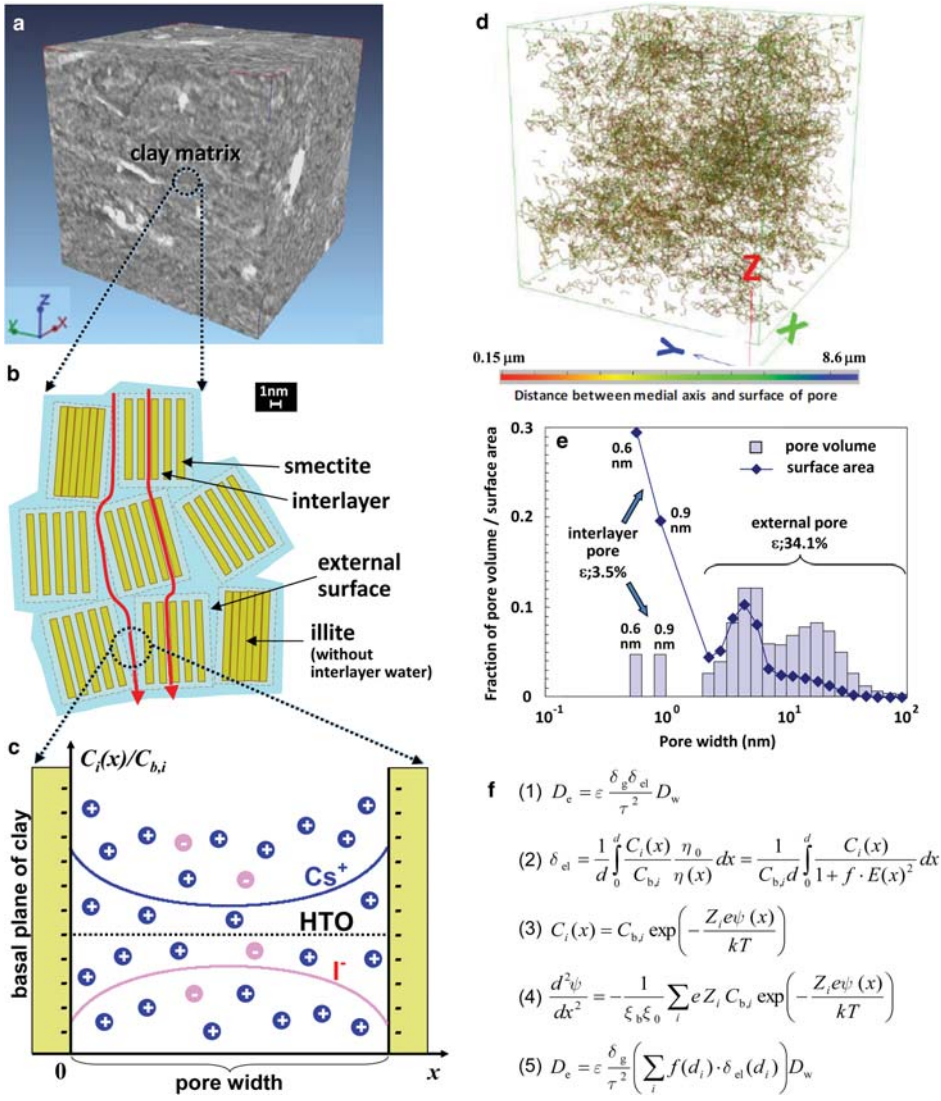

Figure 3. Conceptual images of diffusion model: (a,d) 3D images obtained by nano-focus X-ray CT and medial axis analysis; (b,c) simplified sketch of clay matrix and EDL in narrow pores; (e) pore-size distribution, and (f) equations of EDL diffusion model.

the disparity between the modeled and the measured D_e values of cations may be caused by different diffusion mechanisms based on the ionic properties of each cation.

From these experimental and modeling results, electrostatic interaction at charged surfaces in clays with nanoscale pores can control ionic diffusion of various RNs.

The clay-based modeling approach can essentially be applied in the prediction of diffusion and sorption behaviors of various RNs with complex chemistry, although some systematic gaps in the modeling results need to be evaluated by considering uncertainties in both the experimental and the modeling approaches.

Acknowledgments

This study was conducted partly as 'The project for validating assessment methodology in a geological disposal system' funded by the Ministry of Economy, Trade and Industry of Japan. The authors appreciate contributions by Mitsubishi Materials Corporation and Tokyo Nuclear Service Inc. for experimental work.

Guest editor: Reiner Dohrmann

The authors and editors are grateful to anonymous reviewers who offered very helpful input and suggestions. A list of all reviewers is given at the end of the Preface for this volume.

References

Appelo, C.A.J., Van Loon, L.R., and Wersin, P. (2010) Multicomponent diffusion of a suite of tracers (HTO, Cl, Br, I, Na, Sr, Cs) in a single sample of Opalinus clay. *Geochimica et Cosmochimica Acta,* **74**, 1201–1219.

Bradbury, M.H. and Baeyens, B. (2005) Modelling the sorption of Mn(II), Co(II), Ni(II), Zn(II), Cd(II), Eu(II), Am(III), Sn(IV), Th(IV), Np(V) and U(VI) on montmorillonite: Linear free energy relationships and estimates of surface binding constants for some selected heavy metals and actinides. *Geochimica et Cosmochimica Acta*, **69**, 875–892.

Bradbury, M.H. and Baeyens, B. (2009a) Sorption modelling on illite. Part I: Titration measurements and the sorption of Ni, Co, Eu and Sn. *Geochimica et Cosmochimica Acta*, **73**, 990–1003.

Bradbury, M.H. and Baeyens, B. (2009b) Sorption modelling on illite. Part II: Actinide sorption and linear free energy relationships. *Geochimica et Cosmochimica Acta*, **73**, 1004–1013.

Gorgeon, L. (1994) Contribution à la modelisation physico-chimique de la retention de radioéléments à vie longue par des materiaux argileux. PhD thesis, Université Paris 6.

Japan Atomic Energy Agency (JAEA) (2007) Horonobe underground research laboratory project. Synthesis of phase I investigation 2001–2005. Volume "Geological disposal research". JNC technical report, JAEA-Research 2007-045.

Japan Atomic Energy Agency (JAEA) (2013) Assessment methodology development of chemical effects on geological disposal system. H24 report of Japanese project entrusted by the METI of Japan.

Kitamura, A., Fujiwara, K., Doi, R., Yoshida, Y., Mihara, M., Terashima, M., and Yui, M. (2010) JAEA thermodynamic database for performance assessment of geological disposal of high-level radioactive and TRU wastes. JAEA technical report, JAEA-Data/Code 2009-024.

Leroy, P., Revil, A., and Coelho, D. (2006) Diffusion of ionic species in bentonite. *Journal of Colloid and Interface Science,* **296**, 248–255.

Marques Fernandes, M., Baeyens, B., and Bradbury, M.H. (2008) The influence of carbonate complexation on lanthanide/actinide sorption on montmorillonite. *Radiochimica Acta*, **96**, 691–697.

Marques Fernandes, M., Vér, N., and Baeyens, B. (2015) Predicting the uptake of Cs, Co, Ni, Eu, Th and U on argillaceous rocks using sorption models for illite. *Applied Geochemistry*, **59**, 189–199.

Missana, T., Alonso, U., and Garcia-Gutierrez, M. (2009) Experimental study and modeling of selenite sorption onto illite and smectite clays. *Journal of Colloid and Interface Science*, **334**, 132–138.

NEA (2012) NEA Sorption Project. Phase III: Thermodynamic sorption modeling in support of radioactive waste disposal safety cases. OECD-NEA, Paris.

Parkhurst, D.L. and Appelo, C.A.J. (1999) User's guide to PHREEQC (ver.2) – a computer program for speciation, batch-reaction, one-dimensional transport, and inverse geochemical calculations. U.S. Geological Survey, Water-resouces investigations report 99-4259.

Poinssot, C., Baeyens, B., and Bradubury M.H. (1999) Experimental studies of Cs, Sr, Ni and Eu sorption on Na-illite and the modeling of Cs sorption. PSI technical report, 99006.

Rabung, Th., Pierret, M.C., Bauer, A., Geckeis, H., Bradbury, M.H., and Baeyens, B. (2005) Sorption of Eu(III)/Cm(III) on Ca-montmorillonite and Na-illite Part 1: Batch sorption and time resolved laser fluorescence spectroscopy experiments. *Geochimica et Cosmochimica Acta*, **69**, 5393–5402.

Scheidegger, A.M., Strawn, D.G., Lamble, G.M., and Sparks, D.L. (1998) The kinetics of mixed Ni-Al hydroxide formation on clay and aluminum oxide minerals: A time-resolved XAFS study. *Geochimica et Cosmochimica Acta*, **62**, 2233–2245.

Shibutani, T., Kohara, Y., Oda, C., Kubota, M., Kuno, Y., and Shibata, M. (1999) Physicochemical characteristics of purified Na-smectite and protonation/deprotonation behavior of smectite surface in NaCl media. JNC technical report, JNC TN8400 99-066.

Strawn, D.G. and Sparks, D.L. (2000) Effects of soil organic matter on the kinetics and mechanisms of Pb(II) sorption and desorption in soil. *Soil Science Society of America Journal*, **64**, 144–156.

Tachi, Y. and Yotsuji, K. (2014) Diffusion and sorption of Cs^+, Na^+, I^- and HTO in compacted sodium montmorillonite as a function of porewater salinity: Integrated sorption and diffusion model. *Geochimica et Cosmochimica Acta*, **132**, 75–93.

Tachi, Y., Nakazawa, T., Ochs, M., Yotsuji, K., Suyama, T., Seida, Y., Yamada, N., and Yui, M. (2010) Diffusion and sorption of neptunium(V) in compacted montmorillonite: effects of carbonate and salinity. *Radiochimica Acta*, **98**, 711–718.

Tachi, Y., Yotsuji, K., Seida, Y., and Yui, M. (2011) Diffusion and sorption of Cs^+, I^- and HTO in samples of the argillaceous Wakkanai Formation from the Horonobe URL, Japan: Clay-based modeling. *Geochimica et Cosmochimica Acta*, **75**, 6742–6759.

Tachi, Y., Ochs, M., and Suyama, T. (2014a) Integrated sorption and diffusion model for bentonite. Part 1: Clay–water interaction and sorption modeling in dispersed systems. *Journal of Nuclear Science and Technology*, **51**, 1177–1190.

Tachi, Y., Yotsuji, K., Suyama, T., and Ochs, M. (2014b) Integrated sorption and diffusion model for bentonite. Part 2: Porewater chemistry, sorption and diffusion modeling in compacted systems. *Journal of Nuclear Science and Technology*, **51**, 1191–1204.

Takahashi, H., Seida, Y., and Yui, M. (2009) 3D X-ray CT and diffusion measurements to assess tortuosity and constrictivity in a sedimentary rock. *Diffusion-fundamentals.org 11*, **89**, 1–11.

Tertre, E., Berger, G., Castet, S., Loubet, M., and Giffaut, E. (2005) Experimental sorption of Ni^{2+}, Cs^+ and Ln^{3+} onto a montmorillonite up to 150°C. *Geochimica et Cosmochimica Acta*, **69**, 4937–4948.